UDC 629.783

DOI: 10.20535/2523-4455.mea.338666

Modeling Earth's Magnetic Field for PolyITAN-12U Attitude Determination and Control

D. V. Serhieiev[f], 0000-0001-5613-4874
Ye. Yu. Kovalenko[s], PhD, Assoc. Prof., 0000-0003-1249-2076
Department of Electronic Devices and Systems
National Technical University of Ukraine "Igor Sikorsky Kyiv Polytechnic Institute" 00syn5v21
Kyiv, Ukraine

Abstract—This paper presents a simulation workflow that couples a Keplerian orbit propagator and the World Magnetic Model to generate along-track magnetic-field predictions for typical CubeSat LEO missions. The satellite position estimation mechanism was validated against International GNSS Service reference data, demonstrating acceptable day-scale accuracy that's fit for attitude determination and control system (ADCS) studies. The synthesized geomagnetic environment shows field magnitudes spanning 18.3-51.7 μT (mean 36.2 μT) and rate of change up to 115.4 nT/s, which directly informs magnetometer dynamic-range and sampling requirements. Using measured PolyITAN-12U coil parameters and the spacecraft inertia, those conditions were translated into magnetorquer performance: torques about 2.3×10^{-5} yield angular accelerations of a few $\times10^{-5}$ rad/s² depending on axis and local field strength. The workflow thus provides a quantitatively grounded basis for planning Helmholtz cage hardware-in-the-loop tests and tuning ADCS controllers for PolyITAN-12U satellite.

Keywords — CubeSat; attitude control; magnetic field; orbit propagation

I. INTRODUCTION

CubeSats, modular nanosatellites built around standardized units (1U to 12U) 10x10x10 cm at size each [1], have transformed access to space by drastically reducing development time and cost while enabling focused scientific, Earth-observation, and technology-demonstration missions. Launch expenses have also fallen since such satellites are launched in groups as secondary payloads, further lowering barriers to orbit. Together, these factors have led to a pronounced post-2012 surge in number of CubeSats created by private companies, universities and research organizations [2]. Igor Sikorsky Kyiv Polytechnic Institute was no exception, launching the first satellite of its PolyITAN series in 2014 and now bringing the PolyITAN-12U spacecraft, focused on Earth remote-sensing, to the final stages of development. Despite their small form factor and tight resource budgets in power, mass and volume, modern CubeSats are expected to deliver precise pointing, stable imaging, and repeatable experiments in low Earth orbit. Meeting these mission requirements hinges on reliable knowledge of the satellite's attitude and the ability to regulate it against environmental disturbances.

Attitude Determination and Control Systems (ADCS) thus play a central role in CubeSat performance. Accurate attitude knowledge enables payload boresight pointing, high-gain antenna alignment, optimal solar panels orientation and thermal management strategies. Magnetometers and magnetorquers have a long heritage in small-satellite attitude control [3]. Three-axis magnetometers provide continuous, low-power measurements of the local geomagnetic field, which, when compared to a model of Earth's field, can be used for attitude determination. Magnetorquers, current-driven coils producing a magnetic dipole, interact with Earth's field to generate control torques for detumbling, coarse pointing, and momentum management. This approach is attractive for CubeSats because it is mechanically simple, highly reliable, and propellant-free.

Robust development of such ADCS architectures relies on multi-level verification that covers software-in-the-loop (SIL) and hardware-in-the-loop (HIL) testing [4]. SIL integrates flight software with high-fidelity models of the environment, dynamics, sensors and actuators, enabling early and safe evaluation of algorithms, parameter sensitivities and fault response. HIL complements this by placing real flight hardware, on-board computer, magnetometers and magnetorquer, into a real-time simulation. For magnetic ADCS specifically, HIL often incorporates a Helmholtz-coil cage to reproduce commanded field vectors and dynamics, while injecting realistic

DOI: 10.20535/2523-4455.mea.338666

sensor noise, bias, misalignment, quantization, and other non-idealities.

These practices create a clear need for a rigorous simulation model that couples orbital motion with the surrounding geomagnetic environment. Further in this article, the main elements for constructing such a model are examined, namely, the coordinate systems used in the tasks of spacecraft attitude determination, the orbit-propagation algorithm for an artificial Earth satellite, as well as existing models of Earth's magnetic field. Next, simulation results obtained in MATLAB are presented and a validation method that compares predicted satellite positions with International GNSS Service (IGS) reference data is proposed. In the end, the maximum capabilities of the PolyITAN-12U magnetorquer under real orbit conditions are assessed to demonstrate the practical utility of the simulation results.

II. Methods

A. Coordinate systems

Attitude determination is the process of finding a spacecraft's orientation (attitude) relative to a chosen coordinate system. In practice, multiple coordinate frames are used: an inertial frame for orbital motion, Earth-fixed frames for ground references, local orbital frames for Earth-pointing, and the spacecraft's own body frame. The key coordinate systems are described below.

Earth-Centered Inertial (ECI) frame has its origin at Earth's center, with the Z-axis aligned with Earth's rotational axis pointing toward the north celestial pole, and the X-axis pointing toward the vernal equinox (Fig. 1). The Y-axis completes the right-handed coordinate system. Vernal equinox is the point where the Sun's apparent path (the ecliptic) crosses the celestial equator as it moves from south to north. This frame is considered inertial because it does not rotate with Earth and serves as the primary reference for celestial object directions,

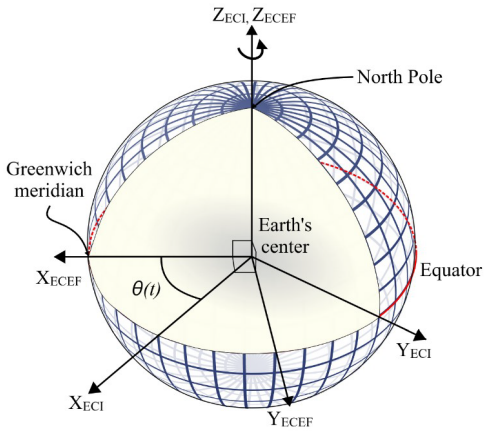

Fig. 1. ECI and ECEF reference frames

especially sun vectors, which are critical for sun sensor operation and optimal solar panel pointing [5].

Earth-Centered Earth-Fixed (ECEF) frame is a terrestrial, rotating reference system defined by the World Geodetic System 1984 (WGS84) standard [6]. Its origin is at Earth's center, the X-axis lies in the equatorial plane and points toward the Greenwich meridian, the Z-axis aligns with Earth's rotational axis, and the Y-axis forms a right-handed system [5]. ECEF is essential for representing Earth-referenced coordinates in satellite ADCS, and is also highly useful for ground-based applications such as ground station communication, accurate antenna pointing, and satellite tracking. Furthermore, ECEF serves as the intermediate frame for transforming between inertial (ECI) and Earth-fixed coordinates [7], typically using the Earth Rotation Angle (ERA) θ:

$$\begin{pmatrix} X_{ECEF} \\ Y_{ECEF} \\ Z_{ECEF} \end{pmatrix} = \begin{pmatrix} X_{ECI} \\ Y_{ECI} \\ Z_{ECI} \end{pmatrix} \cdot \begin{pmatrix} \cos\theta & \sin\theta & 0 \\ -\sin\theta & \cos\theta & 0 \\ 0 & 0 & 1 \end{pmatrix}$$

ERA is a function of time and can be calculated as follows:

$$\theta(t) = 2\pi(0.7790572732640 + 1.00273781191135448 \cdot t),$$

where t is Julian UT1 date minus 2451545.0 or days since J2000.0 epoch.

Geodetic coordinate system specifies positions on or near Earth's surface by latitude φ, longitude λ, and ellipsoidal height h with respect to a chosen reference ellipsoid that best approximates Earth's shape (e.g., WGS-84) [6]. Unlike Cartesian frames, it is tied to a curved reference surface: φ is the angle between the ellipsoid normal at the point and the equatorial plane, measured positive northward from 0° to ±90°, λ is the angle between the point's meridian and the prime meridian, measured positive eastward from 0° to ±180°, and h is the perpendicular distance from the point to the reference ellipsoid surface along the ellipsoidal normal. The geodetic coordinate system serves as the natural interface between satellite orbital mechanics and Earth-based geophysical models, as it directly corresponds to the geographical locations where geophysical phenomena are measured and catalogued. The transformation between ECEF and geodetic coordinate systems requires reference ellipsoid characteristics [7] such as semi-major axis $a = 6378137\ m$, flattening parameter $1/f = 298.257223563$ and some useful derived parameters:

$$e = \sqrt{2f - f^2}$$
$$N(\varphi) = \frac{a}{\sqrt{1 - (e \cdot \sin\varphi)^2}}$$

Here e is the eccentricity, and $N(\varphi)$ is the distance from the surface to the Z-axis in the downward direction, called the Normal Distance. ECEF coordinates are obtained from geodetic via:

DOI: 10.20535/2523-4455.mea.338666

$$X_{ECEF} = (N(\varphi) + h)\cos\varphi\cos\lambda$$
$$Y_{ECEF} = (N(\varphi) + h)\cos\varphi\sin\lambda$$
$$Z_{ECEF} = [N(\varphi)\cdot(1-e^2) + h]\sin\varphi$$

This transformation is exact. The inverse transformation is not so simple, since finding the latitude requires solving a quartic equation [7]. Although direct solutions exist, a more general approach is to use iterative methods. One of them utilizes the following approximation for the transformation:

$$\varphi = \arctan\left(\frac{Z_{ECEF}}{\sqrt{X_{ECEF}^2 + Y_{ECEF}^2}}\cdot\frac{1}{(1-f)^2}\right)$$
$$\lambda = \arctan\left(\frac{Y_{ECEF}}{X_{ECEF}}\right)$$
$$h = \sqrt{X_{ECEF}^2 + Y_{ECEF}^2 + Z_{ECEF}^2} - a \cdot \sqrt{\frac{1-e^2}{1-e^2\cdot\cos\left(\arctan\left(\frac{Z_{ECEF}}{\sqrt{X_{ECEF}^2 + Y_{ECEF}^2}}\right)\right)^2}}$$

Once the approximate values are found, they are converted back into ECEF coordinates. The error is calculated, the initial values are adjusted, and a new estimate is determined. The process continues until the error is reduced to a specified level.

To describe the orientation of a satellite, two local coordinate systems are used: the **Local Vertical Local Horizontal (LVLH)** frame and the satellite's **body frame** (Fig. 2). They both have their origin at the spacecraft's center of mass and rotate with the satellite along its orbit. In LVLH reference system the Z-axis points toward the Earth's center (nadir direction), the X-axis aligned with the spacecraft's velocity vector and the Y-axis completes a right-handed triad [5].

Body frame is anchored to a physical part of the spacecraft chassis and serves as the basis from which onboard subsystems derive their positions [5]. The Z-axis is usually aligned with the main functional direction of the satellite (for example, along the axis of an antenna or camera), the X-axis is perpendicular to the Z-axis, often lying in the plane of symmetry, and the Y-axis completes a right-handed system. For satellite attitude operations such as pointing antennas and instruments toward Earth or a specific ground region, it is necessary to determine the relative orientation between the LVLH and the body frames. This orientation is typically expressed using Euler angles or represented by a direction cosine matrix (DCM) [8].

The last coordinate system to consider is the **North-East-Down (NED)** frame, a local tangent-plane system similar to LVLH but with slightly different directions of axes: X toward geodetic north, Y toward east and Z pointing downward along the gravity (nadir) vector. For attitude control, NED is especially useful because most models of the Earth's magnetic field have their output in local North–East–Down components, enabling straightforward comparison with measurements once transformed to the same frame. Transformations are obtained by rotating to LVLH (or body frame) using spacecraft's orbital geometry to construct the local rotation matrix.

B. *Orbit propagation*

Orbit propagation is the process of predicting a satellite's position in space and velocity over time from a specified initial state, while accounting for various perturbing forces. The satellite's orbit is elliptical, with the Earth at one focus, and is fully described by a set of parameters known as **orbital elements**. These include six key values, commonly referred to as classical or Keplerian elements (Fig. 3): the semi-major axis, eccentricity, orbital inclination, longitude of the ascending node, argument of periapsis, and mean anomaly [9].

The **semi-major axis** a determines the size of the orbit and represents half the maximum distance between the periapsis (the closest point to the central body) and the apoapsis (the farthest point from the central body) of an elliptical orbit. It plays a key role in the satellite's orbital period, as described by Kepler's third law [9]. **Eccentricity** e defines the shape of the orbit

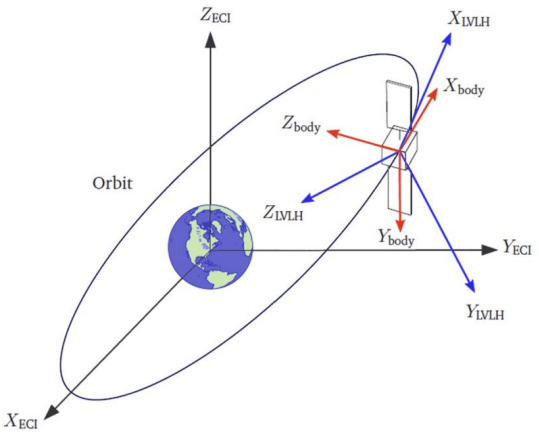

Fig. 2. LVLH and body frame

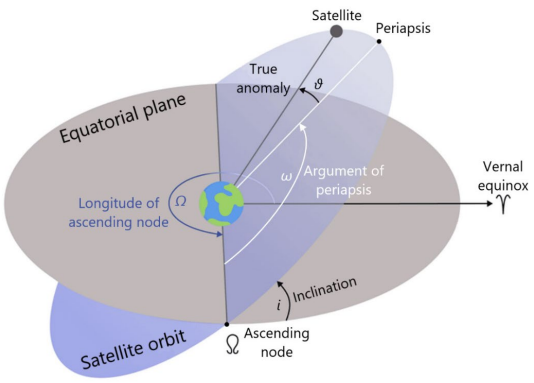

Fig. 3. Keplerian orbital elements

DOI: 10.20535/2523-4455.mea.338666

and measures how much it deviates from a perfect circle. For circular orbits, $e = 0$, while for elliptical ones, $0 < e < 1$. **Inclination** $\boldsymbol{i}$ is the angle between the orbital plane and Earth's equatorial plane. It indicates how tilted the orbit is relative to the equator and determines the satellite's geographic coverage. The **longitude of the ascending node** $\boldsymbol{\Omega}$ is the angle between the direction of the vernal equinox and the ascending node – the point where the satellite crosses the equatorial plane from south to north. The **argument of periapsis** $\boldsymbol{\omega}$ is the angle between the ascending node and the orbit's closest point to Earth (the pericenter). The **mean anomaly** $\boldsymbol{M}$ at a given time t indicates the satellite's position along its orbit at a specific moment.

Today, orbital elements for a specific satellite can be obtained in the form of a Two-Line Element set (TLE) from open databases like CelesTrak or Space-Track. TLE set is a strict, fixed-width text format that encodes both satellite's orbital elements for propagation and some administrative information such as the NORAD catalog number, the International Designator and the epoch specifying when the elements are valid. TLEs are optimized for simplicity and distribution, are most accurate near their epoch, and can diverge quickly for high-drag or maneuvering satellites [10].

Most CubeSats fly in low Earth orbit (LEO), typically 400-600 km altitude, with orbital periods of about 90–97 minutes. Common inclinations are sun-synchronous (97-98°) from rideshare launches, or 51.6° from International Space Station (ISS) deployments at 400-420 km [2]. Lifetimes range from a few months (ISS-like altitudes) to several years near 550–650 km, driven mainly by atmospheric drag. Sun-synchronous orbit (SSO) provides repeatable local time of day for imaging and power, while ISS orbits offer low-cost, frequent access. A minority of CubeSats fly beyond LEO as mission-specific exceptions.

A two-body Keplerian orbit propagator is the simplest but still accurate algorithm to predict trajectory of celestial objects. A satellite's orbital motion is described as the movement of a celestial body influenced by the gravitational field of the planet it orbits [9]. According to Kepler's and Newton's laws, this motion follows an elliptical trajectory, although in many cases, the orbit may be nearly circular. Let's explore the key aspects of satellite flight in orbit.

If the satellite's orbit is assumed to be circular, the distance r from the satellite to the planet's center remains constant. Under these conditions, the satellite moves in uniform rotation around the planet's center, as the gravitational force F acting on it is constant. This gravitational force serves as the centripetal force that keeps the satellite on its circular trajectory [8].

$$\mathrm{F} = \frac{\mathrm{GMm}}{\mathrm{r}^2} = \frac{\mathrm{mv}^2}{\mathrm{r}},$$

where v is the satellite's orbital velocity, $\mathrm{G} = 6{,}673 \cdot 10^{-11}\ \frac{\mathrm{N \cdot m^2}}{\mathrm{kg^2}}$ is the gravitational constant, $\mathrm{M} = 5{,}974 \cdot 10^{24}$ kg is Earth's mass, m is the satellite's mass, and r is the orbital radius. The satellite's velocity is given by the following equation:

$$\mathrm{v} = \sqrt{\frac{\mathrm{GM}}{\mathrm{r}}}$$

Thus, the satellite's speed depends only on its orbit's parameters, particularly its altitude, rather than its mass [8]. The orbital period can then be determined using the following formula:

$$\mathrm{T} = \frac{2\pi \mathrm{r}}{\mathrm{v}} = 2\pi \mathrm{r}\sqrt{\frac{\mathrm{r}}{\mathrm{GM}}} = 2\pi\sqrt{\frac{\mathrm{r}^3}{\mathrm{GM}}}$$

For a more accurate determination of the satellite's coordinates, the elliptical shape of the orbit must be taken into account (Fig. 3). In this case, the length of the radius vector r between the Earth's center and the satellite is not constant, nor is the orbital velocity v. The satellite speeds up as it moves closer to Earth and slows down as it moves farther away. This motion is described by Kepler's equation, which introduces three types of anomalies [9].

The **true anomaly** $\boldsymbol{\vartheta}$ is the angle between the satellite's radius vector r and the direction of the periapsis (Fig. 4). The **mean anomaly** $\mathbf{M}$ is an imaginary angle representing how far the satellite's radius vector r would have rotated if the satellite moved along a circular orbit with a radius equal to the semi-major axis a. The **eccentric anomaly** $\mathbf{E}$ is a parameter used to express variations in the length of the radius vector r.

The eccentric anomaly E and the mean anomaly M are connected through Kepler's equation [9] for an elliptical orbit:

$$\mathrm{M} = \mathrm{E} - \mathrm{e}\sin\mathrm{E} = \mathrm{n}(\mathrm{t} - \mathrm{t}_0),$$

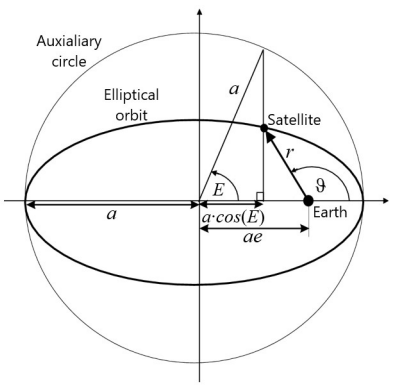

Fig. 4. Motion along an elliptical orbit

DOI: 10.20535/2523-4455.mea.338666

where e is the orbit's eccentricity, t is time, t_0 is the moment the satellite passes through periapsis, and n is the mean motion, given by:

$$n = \frac{2\pi}{T} = \sqrt{\frac{GM}{a^3}}$$

Since Kepler's equation is transcendental (meaning it cannot be solved algebraically for E), numerical methods such as Newton's method are used to approximate its solution [11]. The true anomaly ϑ is related to the eccentric anomaly E by:

$$\operatorname{tg}\frac{\vartheta}{2} = \sqrt{\frac{1+e}{1-e}} \cdot \operatorname{tg}\frac{E}{2}$$

Using these equations along with the classical orbital elements, the true anomaly $\vartheta(t)$ can be expressed as a function of time. To determine how the satellite's radius vector r(t) changes over time, the equation of an ellipse in polar coordinates is used:

$$r = \frac{a(1-e^2)}{1+e\cos\vartheta}$$

In order to go from the radius vector and true anomaly to the satellite coordinates in the ECI reference frame, the following transformations must be performed [12]:

$$x(t) = r(t)[\cos\Omega\cos u(t) - \sin\Omega\sin u(t)\cos i],$$
$$y(t) = r(t)[\sin\Omega\cos u(t) + \cos\Omega\sin u(t)\cos i],$$
$$z(t) = r(t)[\sin u(t)\sin i],$$

where $u(t) = \omega + \vartheta(t)$ is the argument of latitude.

The equations above provide the foundation for describing orbital motion under the influence of a central body's gravity. However, they assume that orbital elements remain constant, which is not always the case. In reality, various factors can cause these parameters to change over time, including:

- **Gravitational perturbations** from other celestial bodies (such as the Moon, the Sun, or other planets) and irregularities in Earth's gravitational field, which is not perfectly uniform.
- **Atmospheric drag.** Satellites in low Earth orbit (typically below 1000 km) experience resistance from the remnants of Earth's atmosphere, gradually lowering their altitude—a process known as orbital decay.
- **Solar radiation pressure.** Sunlight exerts a small but continuous force on a satellite, particularly if it has large solar panels.

To account for these effects and improve accuracy in predicting a satellite's trajectory, more advanced mathematical models and numerical methods are used. One of them is Simplified General Perturbations 4 (SGP4), which incorporates Earth's oblateness and atmospheric drag. However, the Keplerian and SGP4 predictions agree closely over a short simulation period, with differences becoming appreciable only after several days [13]. Therefore, at this stage, the first of them is used.

C. Earth's magnetic field modeling

Earth's magnetic field plays a crucial role in spacecraft attitude control within near-Earth space. In popular algorithms such as TRIAD, the magnetic field vector measured by magnetometer is compared against the model-predicted geomagnetic vector at the satellite's current orbital position to estimate its orientation [4]. A variety of mathematical models capable of predicting magnetic field properties at any given point on or near the planet's surface are currently used. The simplest of these is the **dipole model** [14], which treats Earth as a giant magnetic dipole centered at the planet's geometric center, while its magnetic poles are offset from the geographic poles.

Despite its simplicity and convenience, the dipole model is only an approximation of Earth's actual magnetic field. In reality, the field has a complex structure that includes higher-order variations, described by more advanced models such as the **World Magnetic Model (WMM)** [15] or **International Geomagnetic Reference Field (IGRF)** [16]. Notably, significant local deviations in the magnetic field arise from anomalies in Earth's crust and variations in the outer magnetosphere (Fig. 5). Although IGRF and WMM exhibit comparable accuracy [17], last one is designed for operational navigation and is more commonly used in spacecraft attitude control. Accordingly, WMM is selected for this simulation.

The World Magnetic Model (WMM) is jointly developed by the U.S. National Centers for Environmental Information (NCEI) and the British Geological Survey (BGS) and is updated every five years. It incorporates magnetic measurements from multiple sources, including satellite observations, ground-based magnetometer networks, and oceanographic surveys [15]. According to this model, Earth's magnetic field B can be written in geodetic coordinates as the negative spatial gradient

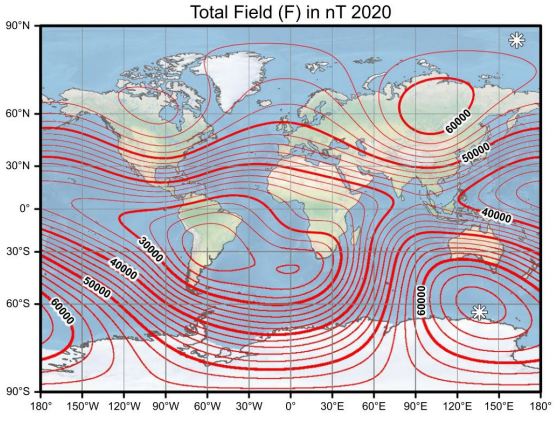

Fig. 5. Map of total field for epoch 2020

DOI: 10.20535/2523-4455.mea.338666

of a scalar potential V, which may be further expanded in terms of spherical harmonics:

$$B(\lambda,\varphi,r,t) = -\nabla V(\lambda,\varphi,r,t),$$
$$V(\lambda,\varphi,r,t) = R_E \sum_{n=1}^{12} \left(\frac{R_E}{r}\right)^{n+1} \sum_{m=0}^{n} (g_n^m(t)\cos(m\lambda) + h_n^m(t)\sin(m\lambda))\breve{P}_n^m(\sin\varphi),$$

where $R_E = 6\,371\,200\ m$ is the radius of the Earth, r is the geocentric distance, λ is the latitude, φ is the longitude, g_n^m and h_n^m are the time-dependent Gauss coefficients of degree n and order m, $\breve{P}_n^m(\mu)$ are the Schmidt semi-normalized associated Legendre functions defined as:

$$\breve{P}_n^m(\mu) = \begin{cases} \sqrt{2\frac{(n-m)!}{(n+m)!}}P_n^m(\mu) \ \ if \ \ m > 0 \\ P_n^m(\mu) \ \ if \ \ m = 0 \end{cases}$$
$$P_n^m(\mu) = (1-\mu^2)^{\frac{m}{2}}\frac{d^m}{d\mu^m}P_n(\mu)$$
$$P_n(\mu) = \frac{1}{2^n n!}\frac{d^n}{d\mu^n}(\mu^2-1)^n$$

The magnetic field vector in the NED reference frame consisting of an eastern component B_X, a northern component B_Y and a vertical component B_Z, is calculated using a set of mathematical equations:

$$B_X = -\frac{1}{r}\frac{\partial V}{\partial \varphi}, \qquad B_Y = -\frac{1}{r\cos\varphi}\frac{\partial V}{\partial \lambda}, \qquad B_Z = \frac{\partial V}{\partial r}.$$

The WMM is a highly accurate tool, but its predictive accuracy decreases over time due to the dynamic nature of Earth's magnetic field. For example, the north magnetic pole has shifted significantly over the past decades, which was one of the reasons for the off-cycle model update in 2020. In addition, external sources of magnetic field, in particular geomagnetic storms driven by solar activity, can cause short-term deviations that the model does not take into account. These deviations can introduce significant error into the predicted attitude angles when using only the magnetometer system, but the error is greatly reduced by adding readings from other sensors [18].

III. Results and Discussion

To verify the correctness of the orbit propagation algorithm, data on the position of GNSS satellites were used. Such data is distributed in a special format, known as SP3 (Standard Product 3), which was originally proposed by Remondi in the late 1980s for GPS. Later it was adopted and extended within the International GNSS Service (IGS) product suite. An SP3 file is an ASCII record of satellite state information sampled at fixed epochs. After a header that declares the version, epoch count, sampling interval, time system and reference frame, each epoch block lists, for every satellite, Cartesian coordinates in the ECEF frame and a clock correction.

IGS offers Ultra-rapid, Rapid, and Final precise orbit/clock products in SP3, trading latency for accuracy [19]. Ultra-rapid files include observed and predicted halves suitable for near real-time. Rapid and Final products are post-processed combinations with the highest consistency. Although SP3 orbits are derived from GNSS microwave tracking, they are routinely validated with Satellite Laser Ranging (SLR) to GNSS satellites equipped with retro-reflectors. This enables the processed orbits from IGS Final to achieve centimeter-level accuracy (≈ 1-2 cm) [19].

IGS Final SP3 positions for NAVSTAR 83 (USA 440) satellite on 1 May 2025 were compared with results of Keplerian orbit propagator initialized with the corresponding orbital elements obtained from the TLE set at the same time epoch:

- Semi Major Axis: $2.6562 \times 10^7\ m$
- Eccentricity: 5.4703×10^{-4}
- Inclination: $54.9546°$
- Longitude of Ascending Node: $350.6580°$
- Argument of Periapsis: $4.2039°$
- True Anomaly: $344.0198°$

It is nearly circular MEO with 20,200 km altitude and period of 12 hours providing global coverage with two passes per sidereal day over a given longitude band and latitude reach to ±55°. Its ground track is shown in Fig. 6.

Absolute errors in the ECEF X, Y, and Z components, together with the 3-D position error magnitude, were calculated for the orbit-propagated states (Fig. 7). Each axis component exhibits a smooth, near-sinusoidal variation with ≈12 hours characteristic period and phase offsets of ≈90°. The amplitude value reaches 57.6 km. The 3-D position error starts near 58 km and drifts downward over the day to 24 km (mean 39.6). These signatures indicate a coherent, low-frequency discrepancy rather than random noise, which is typical for a phase/timing mismatch. This may be caused by insufficient force modeling in a two-body Keplerian propagation, since it does not take into account Earth's oblateness, lunisolar third-body gravity, and solar radiation pressure. Nevertheless, this algorithm, given its simplicity, provides adequate and fairly accurate data on the position and speed of the satellite, which is more than enough for the tasks of this simulation.

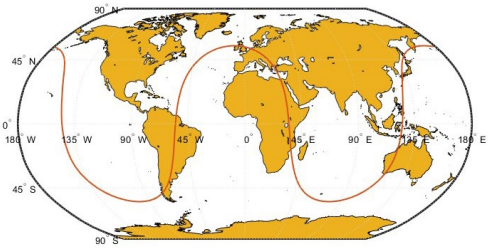

Fig. 6. Ground track of NAVSTAR 83 satellite

DOI: 10.20535/2523-4455.mea.338666

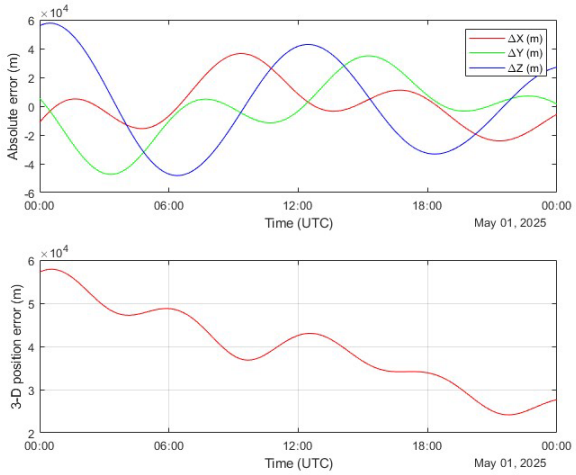

Fig. 7. Error statistics of Keplerian orbit propagation

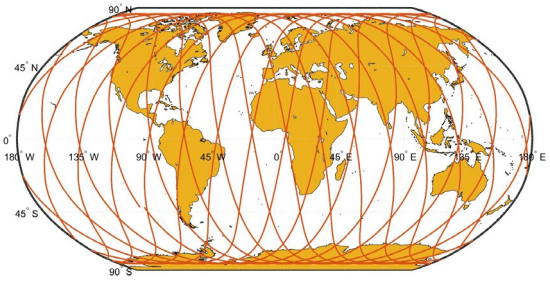

Fig. 8. Ground track of PolyITAN-1 satellite

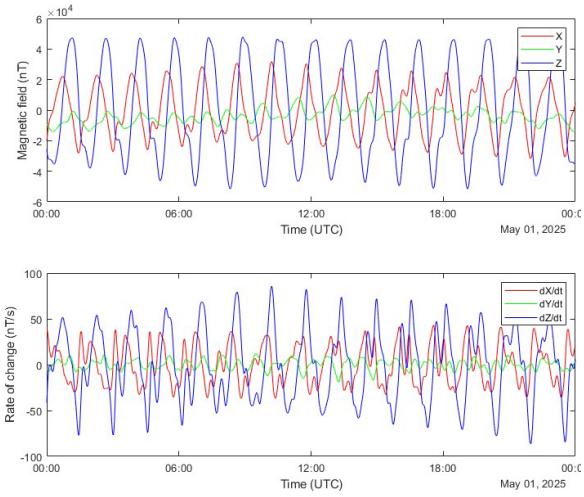

Fig. 9. Earth's magnetic field vector and rate of its change

To study the parameters of the earth's magnetic field that surrounds the satellite during its orbital motion, a series of simulations were conducted using the previously described WMM model. Typical nanosatellite orbits were considered, namely those with a quasi-circular shape (e ≤ 0.005), an altitude of 400-600 km and an inclination of 97-98°. The ground track of PolyITAN-1 satellite, whose orbital elements meet this description, is shown in Fig. 8 as an example:

- Semi Major Axis: $6.8897 \times 10^6\ m$
- Eccentricity: 0.0025
- Inclination: 98.2408°
- Longitude of Ascending Node: 108.2262°
- Argument of Periapsis: 127.7078°
- True Anomaly: 254.8342°

It is a sun-synchronous LEO with a perigee altitude of 494 km and an apogee altitude of 529 km. The satellite completes a revolution in ≈95 minutes (≈15 revolutions per day), providing global coverage of Earth's surface suitable for observation missions.

For each combination of orbital elements, the variation of the magnetic induction vector in three components of the LVLH reference frame and the rate of its change were analyzed (Fig. 9). Based on the results of 518400 simulations, the following conclusions can be drawn. Along the considered orbits, the geomagnetic field magnitude varies from 51.7 μT to 18.3 uT (mean 36.2 uT), while its rate of change associated with the satellite's motion does not exceed 115.4 nT/s.

This data is extremely important and can be used for many different tasks. For example, to calculate the torque generated by a magnetorquer during a real orbital flight. Magnetorquer is one of the most common actuators for CubeSats attitude control, which uses electromagnetic coils or rods to create a magnetic dipole moment [20]:

$$\vec{m} = NIA\hat{n},$$

where N is the number of turns of wire, I is the current provided, A is the effective area of the coil, and $\hat{n}$ is the normal to its plane. The dipole interacts with Earth's magnetic field $\vec{B}$ generating torque:

$$\vec{\tau} = \vec{m} \times \vec{B}$$

The torque changes the satellite's angular momentum, causing rotation about its center of mass (COM) with corresponding angular acceleration [21], which is derived from the Euler equation:

$$\vec{\alpha} = I^{-1}\left(\vec{\tau} - \vec{\omega} \times (I\vec{\omega})\right),$$

where I is moment of inertia tensor in the body frame, $\vec{\omega}$ is angular velocity. If the body spins slowly or only about one principal axis, the cross term of the equation, the gyroscopic coupling, is much smaller than the applied torque and can be ignored:

$$\vec{\alpha} = I^{-1}\vec{\tau}$$

The magnetorquer of the new PolyITAN-12U satellite consists of three coils implemented as four-layer printed circuit boards (PCBs), each mounted to the spacecraft's side panels. This design increases coil area while conserving precious space inside the satellite. The irregular geometry of the coils accommodates panel cut-outs and mounting points and does not affect their performance. An image of the PolyITAN-12U satellite indicating

DOI: 10.20535/2523-4455.mea.338666

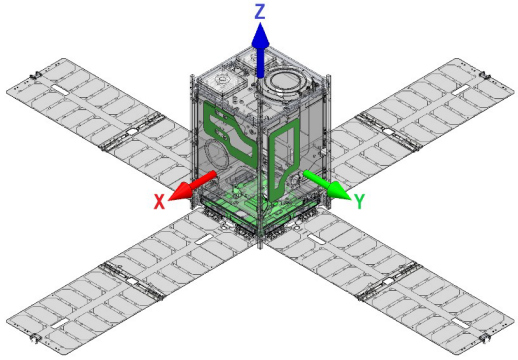

Fig. 10. PolyITAN-12U satellite and its body reference frame

TABLE 1. PARAMETERS OF MAGNETORQUER'S COILS

Parmeter	X	Y	Z
Number of turns	56	56	32
Area, m2	0.0134	0.0136	0.0233
Resistance, Ohm	8.93	9.08	8.96
Nominal current, A	0.829	0.815	0.826
Dipole moment, A·m^2	0.622	0.62	0.616

the body reference frame and coil locations (marked in green) is shown in Fig. 10. Main parameters of the coils are summarized in the Table 1.

PolyITAN-12U uses a 2-cell Li-ion battery bus with a 7.4 V nominal voltage (about 6.0-8.4 V over state-of-charge). Applying the formula given above to the coil parameters provides the magnetic dipole moment they produce, the nominal values of which are also listed in Table 1. The results show that, despite differing coil designs, parameter tuning achieved similar magnetic dipole moments at the same drive current. It should also be noted that the maximum achievable magnetic dipole moment will vary depending on the battery charge level within the range of 0.5 A·m2 to 0.7 A·m^2.

The mass of the satellite is 23.8 kg, its center of mass is shifted relative to the geometric center by the following values: ΔX = 9.2 mm, ΔY = -6.6 mm, ΔZ = 8.1 mm (in the body reference frame). These characteristics fully satisfy the CubeSat Design Specification rev. 14.1 for 12U nanosatellite [1] making it fully compatible with most standardized CubeSat dispensers. The moment of inertia tensor below describes the satellite's mass distribution about the COM and determines its rotational response to applied torques:

$$\mathrm{I} = \begin{bmatrix} I_{xx} & -I_{xy} & -I_{xz} \\ -I_{yx} & I_{yy} & -I_{yz} \\ -I_{zx} & -I_{zy} & I_{zz} \end{bmatrix} = \begin{bmatrix} 0.5043 & -0.0328 & -0.0037 \\ -0.0328 & 0.5155 & -0.0069 \\ -0.0037 & -0.0069 & 0.5268 \end{bmatrix} \mathrm{kg \cdot m^2}$$

The fundamental limitation of a magnetorquer is that the torque it creates is always perpendicular to the external magnetic field, which significantly complicates satellite attitude control. Therefore, several assumptions are made for further calculations. Since the system of three orthogonal coils allows the resulting magnetic dipole moment vector to be oriented in any desired direction, it is commanded to remain at 90° to the geomagnetic field vector in order to maximize the generated torque. The magnitude of this dipole does not exceed that produced by a single coil. Also, the satellite is oriented in such a way that the Earth's magnetic field is directed perpendicular to the rotation axis being studied. Together, these considerations make it possible to assess the maximum capabilities of the PolyITAN-12U magnetorquer during operation in low Earth orbit.

With the maximum recorded geomagnetic field strength of 51.7 μT the magnetorquer can produce 3.2×10^{-5} N·m of torque under nominal operating conditions. Using the inertial characteristics of the satellite given above, this torque values can be converted into the corresponding angular accelerations along each axis of the body reference frame: 6.402×10^{-5} rad/s^2 along X, 6.252×10^{-5} rad/s^2 along Y and 6.045×10^{-5} rad/s^2 along Z. At the orbital location where the geomagnetic field is weakest (18.3 μT), the generated torque drops to 1.13×10^{-5} N·m, corresponding to an angular acceleration of 2.269×10^{-5} rad/s^2 along X, 6.252×10^{-5} rad/s^2 along Y and 6.045×10^{-5} rad/s^2 along Z. Other values obtained for different orbital conditions and magnetorquer operating modes are summarized in the Table 2.

As can be seen from these data, the magnetorquer is capable of producing very small torques and its efficiency is highly dependent on the external magnetic field. For greater clarity, operating for 10 minutes at nominal current and average geomagnetic field strength, the magnetorquer will change the spacecraft's angular velocity by only 0.0264 rad/s or 1.513 °/s while consuming about 1 Wh of energy. Nevertheless, the simplicity of design and integration, as well as high reliability and limited choice of alternative actuators make magnetorquers indispensable for small spacecraft such as CubeSats.

This is far from the only application of the obtained model. In the future, it will be integrated into a broader software-hardware simulation platform enabling comprehensive hardware-in-the-loop (HIL) testing of the spacecraft. Knowledge of the geomagnetic field extremes and the rate of its change along the satellite's orbit enables correct specification of the Helmholtz coil system, which is part of the simulation stand. Additionally, data on the PolyITAN-12U magnetorquer's on-orbit performance limits will help improve existing algorithms for both attitude control and power-management.

DOI: 10.20535/2523-4455.mea.338666

Table 2. Magnetorquer capabilities

Axis (body frame)		X			Y			Z		
Coil current		*min*	*nom*	*max*	*min*	*nom*	*max*	*min*	*nom*	*max*
Max. magnetic field (51.7 μT)	Torque, $\times 10^{-5}$ N·m	2.607	3.215	3.649	2.602	3.209	3.643	2.582	3.184	3.614
	Angular acceleration, $\times 10^{-5}$ rad/s^2	5.191	6.402	7.267	5.069	6.252	7.097	4.901	6.045	6.862
Avg. magnetic field (36.2 μT)	Torque, $\times 10^{-5}$ N·m	1.824	2.249	2.553	1.821	2.245	2.549	1.806	2.228	2.528
	Angular acceleration, $\times 10^{-5}$ rad/s^2	3.632	4.479	5.084	3.547	4.375	4.965	3.429	4.229	4.801
Min. magnetic field (18.3 μT)	Torque, $\times 10^{-5}$ N·m	0.924	1.139	1.293	0.922	1.137	1.291	0.915	1.128	1.281
	Angular acceleration, $\times 10^{-5}$ rad/s^2	1.839	2.269	2.576	1.797	2.216	2.515	1.737	2.143	2.432

Of course there are ways to improve the developed model. The first of them involves upgrading the orbit propagation algorithm to take into account various perturbation factors, which will reduce the error in predicting the satellite position over long simulation periods. Such an upgrade could be a transition to SGP4 or another more advanced algorithm. The second improvement is simulation of external magnetic field sources such as magnetic storms and evaluation of their influence on spacecraft's ADCS operation.

Conclusion

The development of a simulation model that combines the prediction of the satellite's orbital position and the parameters of the Earth's magnetic field surrounding it was carried out in this work. The model couples the Keplerian orbit propagator, which despite its simplicity provides good accuracy over short simulation intervals, and the World Magnetic Model, a periodically (five-year) updated model of Earth's main magnetic field and its secular variation. Validation against IGS reference data showed average 3D-position error of 39.6 km which can be caused by simplified force modeling in chosen orbit propagator, but is still acceptable for solving current tasks. Using this framework, the geomagnetic environment for typical LEO CubeSat orbits (400-600 km, 98°-98° inclination) was quantified: the total field magnitude varies from 51.7 μT to 18.3 uT, and the rate of change along track remains below 115.4 nT/s. Then these environmental limits were mapped to actuator capability for the PolyITAN-12U magnetorquer. Given the coil designs and the satellite's inertia properties, the achievable torque is on the order of 10^{-5} N·m, yielding angular accelerations of a few $\times 10^{-5}$ rad/s^2 depending on axis and local field strength. Consequently, even sustained operation at nominal current produces modest attitude-rate changes, which should be taken into account when developing attitude control and power management algorithms. The obtained results, together with the developed model, will be used to create a comprehensive HIL simulation platform for satellite test and evaluation.

References

[1] A. Johnstone, "CubeSat Design Specification Rev. 14.1," Feb. 2022, **URL:** https://static1.squarespace.com/static/5418c831e4b0fa4ecac1bacd/t/62193b7fc9e72e0053f00910/1645820809779/CDS+REV14_1+2022-02-09.pdf.

[2] E. Kulu, "CubeSats & Nanosatellites - 2024 Statistics, Forecast and Reliability," in *31st IAA Symposium on Small Satellite Missions*, 2024, pp. 601–614, **DOI:** 10.52202/078365-0069.

[3] H. Shim, O.-J. Kim, M. Park, M. Choi, and C. Kee, "Development of Hardware-in-the-Loop Simulation for CubeSat Platform: Focusing on Magnetometer and Magnetorquer," *IEEE Access*, vol. 11, pp. 73164–73179, 2023, **DOI:** 10.1109/ACCESS.2023.3294565.

[4] M. K. Quadrino, "Testing the Attitude Determination and Control of a CubeSat with Hardware-in-the-Loop," Massachusetts Institute of Technology, 2014, **URL:** https://dspace.mit.edu/handle/1721.1/91382.

[5] F. L. Markley and J. L. Crassidis, *Fundamentals of Spacecraft Attitude Determination and Control*. New York, NY: Springer New York, 2014, **ISBN:** 978-1-4939-0801-1. **DOI:** 10.1007/978-1-4939-0802-8_1.

[6] "World Geodetic System 1984," Sep. 1991, **URL:** https://apps.dtic.mil/sti/tr/pdf/ADA280358.pdf.

[7] J. Stryjewski, "Coordinate Transformations," **URL:** https://x-lumin.com/wp-content/uploads/2020/09/Coordinate_Transforms.pdf.

[8] Charles. Brown and W. Software. C Brown, *Elements of Spacecraft Design*. AIAA (American Institute of Aeronautics & Astronautics), 2004. **ISBN:** 978-1563475245

[9] Roger. Bate, D. D. Mueller, and J. E. White, *Fundamentals of astrodynamics*. Dover Publications, Inc., 1971.

[10] P. Cefola, D. A. Vallado, and P. J. Cefola, "Two-line element sets-Practice and use," In 63rd International Astronautical Congress, Naples, Italy, International Astronautical Federation, 2012.

[11] M. Palacios, "Kepler equation and accelerated Newton method," *J Comput Appl Math*, vol. 138, no. 2, pp. 335–346, Jan. 2002, **DOI:** 10.1016/S0377-0427(01)00369-7.

[12] A. Porras-Hermoso, J. Cubas, and S. Pindado, "On the satellite attitude determination using simple environmental models and sensor data," *J Phys Conf Ser*, vol. 2090, no. 1, p. 012116, Nov. 2021, **DOI:** 10.1088/1742-6596/2090/1/012116.

[13] "Comparison of Orbit Propagators," *MATLAB Documentation*. [Online]. Available: https://www.mathworks.com/help/aerotbx/ug/comparison-of-orbit-propagators.html.

[14] M. Navabi and M. Barati, "Mathematical modeling and simulation of the earth's magnetic field: A comparative study of the models on the spacecraft attitude control application," *Appl Math Model*, vol. 46, pp. 365–381, Jun. 2017, **DOI:** 10.1016/j.apm.2017.01.040.

[15] Chulliat *et al.*, "The US/UK World Magnetic Model for 2025-2030: Technical Report," 2025, **DOI:** 10.25923/prbc-s316.

[16] P. Alken *et al.*, "International Geomagnetic Reference Field: the thirteenth generation," *Earth, Planets and Space*, vol. 73, no. 1, p. 49, Dec. 2021, **DOI:** 10.1186/s40623-020-01288-x.

[17] J.-F. Oehler, D. Rouxel, and M.-F. Lequentrec-Lalancette, "Comparison of global geomagnetic field models and evaluation using marine datasets in the north-eastern Atlantic Ocean and western Mediterranean Sea," *Earth, Planets and Space*, vol. 70, no. 1, p. 99, Dec. 2018, **DOI:** 10.1186/s40623-018-0872-y.

[18] D. Cilden-Guler, Z. Kaymaz, and C. Hajiyev, "Geomagnetic disturbance effects on satellite attitude estimation," *Acta Astronaut*, vol. 180, pp. 701–712, Mar. 2021, **DOI:** 10.1016/j.actaastro.2020.12.044.

[19] J. Kouba, "A guide to using International GPS Service (IGS) products," Ottawa, Sep. 2015, **URL:** https://files.igs.org/pub/resource/pubs/UsingIGSProductsVer21_cor.pdf.

[20] A. El Fatimi, A. Addaim, and Z. Guennoun, "Study and design of an active magnetorquer actuator model for nanosatellites," *E3S Web of Conferences*, vol. 351, p. 01051, May 2022, **DOI:** 10.1051/e3sconf/202235101051.

[21] S. B. Örs, "Developing an Attitude Determination and Control System for 1U CubeSat," Jun. 2024, **DOI:** 10.13140/RG.2.2.35088.42240.

Надійшла до редакції 29 квітня 2025 року
Прийнята до друку 06 серпня 2025 року

DOI: 10.20535/2523-4455.mea.338666

УДК 629.783

DOI: 10.20535/2523-4455.mea.338666

Моделювання магнітного поля Землі для визначення та контролю орієнтації PolyITAN-12U

Д. В. Сергєєв[f], 0000-0001-5613-4874
Є. Ю. Коваленко[s], канд. техн. наук, доцент, 0000-0003-1249-2076
Кафедра електронних приладів та систем
Національний технічний університет України
«Київський політехнічний інститут імені Ігоря Сікорського» 00syn5v21
Київ, Україна

Анотація—У статті представлено симуляційну модель, яка поєднує алгоритм прогнозування орбіти на основі рівняння Кеплера та модель World Magnetic Model, для визначення реальних характеристик магнітного поля Землі на типових для наносупутників CubeSat орбітах (висота 400-600 км, нахил 97-98°). Перевірка правильності обчислення позиції супутника, здійснена за допомогою еталонних значень від International GNSS Service, показала добову точність, достатню для дослідження системи орієнтації та стабілізації. Отримані за результатами численних симуляцій оцінки магнітного середовища лежать у межах від 51.7 мкТл до 18.3 мкТл (середнє значення 36.2 мкТл), а швидкість зміни магнітного поля, пов'язана з переміщенням супутника, не перевищує 115.4 нТл/с. На основі параметрів магнітних котушок PolyITAN-12U та його інерційних характеристик показано, що в умовах реальної орбіти вони здатні створювати обертальні моменти від 1.1×10^{-5} Н·м до 3.2×10^{-5} Н·м, забезпечуючи кутові прискорення від 2.1×10^{-5} рад/с^2 до 6.4×10^{-5} рад/с^2 в залежності від осі, струму котушок та локального магнітного поля. Таким чином, навіть тривала робота на номінальному струмі спричиняє доволі невеликі зміни кутової швидкості апарату, що слід врахувати під час розробки алгоритмів керування орієнтацією та енергоспоживанням. Розроблена модель та отримані числові дані будуть застосовані для побудови повноцінного hardware-in-the-loop тестування PolyITAN-12U з використанням клітки Гельмгольца, що дозволить значно покращити процес відлагодження алгоритмів керування орієнтацією супутника. Також слід зазначити, що запропоновані підходи не враховують такі ефекти як гравітаційні збурення, атмосферний опір та тиск сонячного випромінювання при розрахунку орбіти, а також зовнішні джерела магнітного поля такі як геомагнітні бурі, викликані сонячною активністю. Все це відкриває шлях для подальшого удосконалення моделі.

Ключові слова — CubeSat; керування орієнтацією; магнітне поле; прогнозування орбіти